Carbohydrate Polymers 121 (2015) 79–85

Contents lists available at ScienceDirect

Carbohydrate Polymers

journal homepage: www.elsevier.com/locate/carbpol

Adsorption of uranium by amidoximated chitosan-grafted polyacrylonitrile, using response surface methodology

Chao Xu [1], Jingjing Wang [1], Tilong Yang, Xia Chen, Xunyue Liu, Xingcheng Ding*

Key Laboratory of Chinese Ministry of Agriculture for Nuclear-Agricultural Sciences, Institute of Nuclear-Agricultural Science, Zhejiang University, Hangzhou 310029, PR China

ARTICLE INFO

Article history:
Received 5 September 2014
Received in revised form
30 November 2014
Accepted 2 December 2014
Available online 31 December 2014

Keywords:
Chitosan
Uranium
Polyacrylonitrile
Amidoxime
Response surface methodology (RSM)

Chemical compounds studied in this article:
Chitosan (PubChem CID: 71853)
Acrylonitrile (PubChem CID: 7855)
Hydroxylamine hydrochloride (PubChem CID: 443297)
Uranylnitrate hexhydrate (PubChem CID: 61640)

ABSTRACT

The amidoximated chitosan-grafted polyacrylonitrile (CTS-*g*-PAO) was prepared for the adsorption of uranium from water. The effects of pH, concentration of uranium and the solid–liquid ratio on the adsorption of uranium by CTS-*g*-PAO were optimized using Doehlert design of response surface methodology (RSM). The adsorption capacity and removal efficiency achieved 312.06 mg/g and 86.02%, respectively. The adsorption process attained equilibrium only in 120 min. More than 80% of the absorbed uranium could be desorbed by 0.1 mol/l HCl or EDTA-Na, and CTS-*g*-PAO could be reused at least 3 times. The CTS-*g*-PAO and U(VI) ions formed a chelate complex due to FTIR spectral analysis. The surface morphology of CTS-*g*-PAO was also investigated by SEM. The adsorption process was better described by Langmuir isotherm and pseudo second order kinetic model. Results obtained indicated that CTS-*g*-PAO was very promising in adsorption of uranium from water.

1. Introduction

Chitin/chitosan is the second most abundant natural polysaccharide in the world. Chitosan has been employed in the adsorption of uranium (Oshita, Sabarudin, Takayanagi, Oshima, & Motomizu, 2009; Schleuter et al., 2013) and other metal ions (Varma, Deshpande, & Kennedy, 2004; Wan Ngah, Teong, & Hanafiah, 2011). It is considered to be one of the most promising materials extracting uranium from contaminated water and sea water (Muzzarelli, 2011), for the biocompatibility and the high adsorption capacity of uranium (about 300 mg/g).

However, the high solubility of chitosan in acid solutions and its poor mechanical properties (Rinaudo, 2006), limit its applications in nuclear industry. Some kinds of modified chitosan such as cross-linking and graft copolymerization (Jayakumar, Prabaharan, Reis, & Mano, 2005) have been synthesized to improve its adsorption properties. While toxic reagents, such as glutaraldehyde and epichlorohydrin, were usually required in those procedures of modification (Wan Ngah et al., 2011).

The amidoxime group is also biocompatible and has been applied in the adsorption of metal ions (Gao, Gao, & Li, 2010). For uranium, it is usually used in the extraction from sea-water (Shen, Lin, Chen, Zhou, & Jin, 2011). Most amidoxime materials have good selectivity and mechanical properties in spite of the low adsorption capacity. The combination of chitosan and amidoxime group will make their respective advantages complementary to each other.

Response surface methodology (RSM) is a favorable methodology widely applied in all kinds of engineering courses, i.e. biochemical engineering, food processing and biosorption for optimization (Amini, Younesi, & Bahramifar, 2009; Dotto & Pinto, 2011; Kumar, Singh, Kumar, Bishnoi, & Bishnoi, 2009). This statistical design can well illustrate the interactions of variables and find out the optimum conditions of variables, which are ignored in traditional one-factor design. As one of practical RSM models

* Corresponding author. Tel.: +86 159 0661 9218; fax: +86 571 8697 1201.
E-mail address: dingxch@zju.edu.cn (X. Ding).
[1] These authors contributed equally to this work and should be considered as co-first authors.

http://dx.doi.org/10.1016/j.carbpol.2014.12.024
0144-8617/

the Doehlert model minimizes experimental points and maintains high precision of prediction (Bezerra, Santelli, Oliveira, Villar, & Escaleira, 2008; Doehlert, 1970). It will be more efficiency and comprehensive that making this statistical method applied in the adsorption study of uranium.

In this study, amidoximated chitosan-grafted polyacrylonitrile was prepared for the adsorption of UO_2^{2+} from aqueous solutions. The Doehlert design of RSM was applied to study the influences of initial pH, initial concentration of uranium and the solid–liquid ratio on the adsorption. To test the practicability, desorption and regeneration experiments were also committed. The isotherm and kinetics analysis was completed to identify the adsorption process.

2. Experimental

2.1. Materials

All the chemicals used were of analytical grade. Acrylonitrile (AN) and chitosan (deacetylation: 95%) was procured from Guangfu Fine Chemical Research Institute (Tianjin, China) and Fuli Biological Technology Co. (Zhejiang, China), respectively. $UO_2(NO_3)_2{\cdot}6H_2O$ was obtained from Chushengwei Chemistry Co. (Hubei, China). Arsenazo III was obtained from East China Normal University. Other chemicals, such as $K_2S_2O_8$, $NaHSO_3$ and hydroxylamine hydrochloride, were procured from Sangon biotech.

U_3O_8 was obtained from $UO_2(NO_3)_2{\cdot}6H_2O$ by being fired in muffle furnace at 850 °C for 4 h. The stock solution of U(VI) (1000 mg/L) was prepared by heating and dissolving accurately weighed U_3O_8 in adequate HCl, H_2O_2 and distilled water. Other artificial U(VI) solutions in this study were all diluted from the stock solution.

2.2. Preparation

Chitosan-grafted polyacrylonitrile (CTS-*g*-PAN): The aqueous precipitation graft copolymerization of chitosan and AN was carried out in 1000 ml three-necked flask at 60 °C for 4 h. Chitosan (10 g in 300 ml of 2.5% aq. acetic acid solution) was firstly added into the flask. Then AN (40 ml), $K_2S_2O_8$ (3.75 g in 100 ml of water) and $NaHSO_3$ (0.77 g in 10 ml of water) were pumped into the flask continuously in the rate of 1.0 l/h with constant stirring and ventilating of nitrogen gas. The graft copolymerization was terminated by adding adequate 2 wt% NaOH solution. Then absolute ethyl alcohol (100 ml) was added into the flask as demulsifier. The obtained precipitate was filtered and washed by ethyl and water three times (Lv, Bin, Li, Chen, Wang, & Zhao, 2009; Shankar, Gomathi, Vijayalakshmi, & Sudha, 2014). The product was dried in a vacuum oven at 50 °C and weighed.

The sample was further purified by *N*,*N*-dimethyl formamide using soxhlet extraction method for 4 h to remove any homo polymer. Then the solid sample was dried and weighed again. The grafting and grafting efficiency were calculated by the following equations (Mohamed & Sabaa, 2010):

$$\text{grafting } (\%G) = \left[\frac{(W_1 - W_0)}{W_0}\right] \times 100\% \quad (1)$$

$$\text{grafting efficiency } (\%E) = \left[\frac{(W_1 - W_0)}{W_2}\right] \times 100\% \quad (2)$$

where W_0, W_1 and W_2 are, respectively, the weight of original chitosan, grafted chitosan and the monomer (AN) used.

CTS-*g*-PAO: The CTS-*g*-PAN powder was swelled in methanol for 3 h in advance. The amidoximation of prepared CTS-*g*-PAN (7.21 g) was done by 70 g/l hydroxylamine hydrochloride in methanol/H_2O (v/v = 3:2) solution (400 ml) whose pH was adjusted to 6.5 by NaOH powder. The mixture was stirred at 70 °C for 4 h and then washed by ethyl and water three times (Mohamed & Sabaa, 2010). Then the product was dried in a vacuum oven at 50 °C and weighed. The amidoximation efficiency was calculated by the following equations:

$$\text{amidoximation efficiency} = \frac{[(W_3 - W_1) \times 53.06]}{[(W_1 - W_0) \times 33.03]} \times 100\% \quad (3)$$

where W_3 is the weight of CTS-*g*-PAO.

2.3. Characterization

FTIR spectra of intermediate and final products with and without uranium were recorded by NICOLET AVA TAR370 FTIR spectrometer to test whether the preparation was successful, and which reaction was between absorbing material and uranium.

Scanning electron microscopy (SEM) was also employed to study the microcosmic properties of the absorbing materials before and after the adsorption by HITACHI TM-1000 microscope.

2.4. Adsorption experiments

2.4.1. Uranium determination

The concentration of uranyl ions (UO_2^+ converted to uranium, mg/l) was determined by a UV spectrophotometer (INESA L5s) using arsenazo III at 652 nm (Wang, Peng, Yang, Liu, & Hu, 2011).

The pH of solution was adjusted by 0.1 mol/l NaOH and 0.1 mol/l HCl solutions. CTS-*g*-PAO was added into the prepared uranyl solution. The weight of added CTS-*g*-PAO, the initial pH and initial concentration of uranyl solution varied according to the statistical design. The samples were stirred at 200 rpm for 24 h at room temperature. The uranium adsorption capacity (q) and removal efficiency (e) were calculated by the following equations:

$$q = (C_0 - C_e)\,\frac{V}{M} \quad (4)$$

$$e = \left[\frac{(C_0 - C_e)}{C_0}\right] \times 100\% \quad (5)$$

where C_0 and C_e is, respectively, the initial and equilibrium concentration of uranyl solution, V is the volume of uranyl solution, and M is the weight of absorbing materials.

2.4.2. Statistical design

Response surface methodology (RSM) was used to optimize the adsorption of uranium. A Doehlert design was employed with three independent variables including initial pH (X_1), initial concentration of uranium (X_2) and the solid–liquid ratio (X_3) (Doehlert, 1970). The matrix of design was shown in Table 1, including coded and actual values of the three variables in 15 runs. Every run was an average of triple repetition. The relationship between coded and actual values could be described by the following equation:

$$x = \frac{(X_i - X_0)}{\Delta X} \quad (6)$$

where x is the coded value, X_i is the actual value, X_0 is the actual value at the center point, ΔX is the step change value of the variables (Bezerra et al., 2008).

The quadratic polynomial regression model was used to express the effects of independent variables on responses according to the following equation:

$$Y = b_0 + \sum_{i=1}^{n} b_i x_i + \sum_{i=1}^{n} b_{ii} x_i^2 + \sum_{1 \le i < j}^{n} b_{ij} x_i x_j + \varepsilon \quad (7)$$

where Y is the response, b_0 is the model constant, b_i, b_{ii} and b_{ij} are the coefficients, x_i and x_j are independent variables, n is the amount of variables, and ε is the error. The evaluation and generation of the experimental design was performed with the help of Design-Expert® version 8.0.6 software.

Table 1
Doehlert design matrix of three variables in actual and coded forms along with predicted and observed response.

Run	Initial pH (X_1)	Initial concentration (mg/l) (X_2)	Solid–liquid ratio (mg/l) (X_3)	Adsorption capacity (mg/g)		Removal efficiency (%)	
				Observed	Predicted	Observed	Predicted
1	4.6 (−1)	50 (0)	100 (0)	86.22	85.12	17.24	17.03
2	5.8 (−0.5)	40 (−0.289)	50 (−0.817)	192.19	187.58	24.02	23.84
3	5.8 (−0.5)	60 (0.289)	150 (0.817)	160.10	159.96	40.03	39.33
4	5.8 (−0.5)	20 (−0.866)	100 (0)	108.25	112.39	54.13	55.27
5	5.8 (−0.5)	80 (0.866)	100 (0)	207.82	210.78	25.98	26.79
6	7.0 (0)	70 (0.577)	50 (−0.817)	312.06	319.52	22.29	22.07
7	7.0 (0)	30 (−0.577)	150 (0.817)	172.03	168.09	86.02	86.90
8	7.0 (0)	50 (0)	100 (0)	241.11	236.48	48.22	47.30
9	7.0 (0)	50 (0)	100 (0)	233.84	236.48	46.77	47.30
10	7.0 (0)	50 (0)	100 (0)	234.42	236.48	46.88	47.30
11	8.2 (0.5)	40 (−0.289)	50 (−0.817)	119.65	119.81	14.96	15.23
12	8.2 (0.5)	60 (0.289)	150 (0.817)	110.34	113.11	27.58	27.81
13	8.2 (0.5)	80 (0.866)	100 (0)	133.69	128.83	16.71	16.37
14	8.2 (0.5)	20 (−0.866)	100 (0)	84.19	83.05	42.10	40.84
15	9.4 (1)	50 (0)	100 (0)	37.94	38.45	7.59	7.69

2.4.3. Desorption and regeneration

The CTS-*g*-PAO (20 mg) was added into 200 ml, 85 mg/l uranyl solution at pH = 7.0 at room temperature, and shaken at 200 rpm to equilibrium. The concentration was recorded. CTS-*g*-PAO after adsorption was filtered and dried at 50 °C to constant weight, then added into 100 ml 0.1 mol/l HCl or 0.1 mol/l EDTA-Na solutions and shaken at 200 rpm for 2 h. The concentration of desorption solution was recorded, too. CTS-*g*-PAO was filtered and dried at 50 °C to constant weight again. The above steps were repeated 3 times. The uranium recycle efficiency (R_1) and material regeneration efficiency (R_2) were calculated by the following equations:

$$\text{recycle efficiency}: R_1 = \frac{\text{desorbed uranium}}{\text{adsorbed uranium}} \times 100\% \quad (8)$$

$$\text{regeneration efficiency}: R_2 = \frac{q_i}{q_1} \times 100\% \quad (9)$$

where q_i and q_1 are the adsorption capacity in this run and first run (mg/g, $i > 1$).

2.4.4. Adsorption isotherm and kinetics

For isotherm studies, 10 mg CTS-*g*-PAO was added into 200 ml uranyl solution of different concentrations (15, 30, 45, 70 and 80 mg/l) at pH = 7.0 at room temperature, and shaken at 200 rpm for 24 h. The concentrations after shaking were determined to calculate the adsorption capacity.

For kinetics studies, 25 mg CTS-*g*-PAO was added into 500 ml, 85 mg/l uranyl solution at pH = 7.0 at room temperature, and shaken at 200 rpm. The concentrations of different shaking times (15, 30, 45, 60, 90, 120, 180, 240, 360 and 420 min) were determined to calculate the adsorption capacity.

3. Results and discussion

3.1. Characterization

The amidoximated chitosan-grafted polyacrylonitrile (CTS-*g*-PAO) was prepared according to the method shown in Fig. 1. The chitosan, CTS-*g*-PAN, CTS-*g*-PAO and CTS-*g*-PAO after adsorption of uranium have been taken into FTIR analysis. The sharp peak at 2243 cm^{-1} only appeared in spectrum of CTS-*g*-PAN due to —CN bond (Ning, 2000). It proved that the graft copolymerization of chitosan with acrylonitrile was succeeded. There was an adsorption peak at 932 cm^{-1} only in spectrum of CTS-*g*-PAO, corresponding to the stretching of the —C=N—OH bond. The blue shift appeared at 1646–1651 cm^{-1} in spectra of chitosan and CTS-*g*-PAO, related to the effect of —C=N— bond on $—NH_2$ bond. These three variations all demonstrated that the amidoximation of CTS-*g*-PAN was successful. According to equations 1, 2 and 3, the grafting, grafting efficiency and amidoximation efficiency were 226.51%, 70.13% and 86.08%, respectively, by gravimetric method.

In spectra of CTS-*g*-PAO before and after adsorption, the peak variation from 932 to 913 cm^{-1} was due to the stretching frequency of linear structure of O=U=O (Anirudhan & Radhakrishnan, 2009; Saraydin, Isikver, & Sahiner, 2001) and —C=N—OH bond. It demonstrated that the uranium was assuredly adsorbed by CTS-*g*-PAO. And the red shift from 1651 to 1645 cm^{-1} indicated that the amidoxime group and $—NH_2$ bond took important roles in the adsorption of uranium by CTS-*g*-PAO. It could be inferred from above that uranyl ions was bonded to amidoxime and amino group by chelation.

3.2. Response surface methodology

3.2.1. Analysis of variance (ANOVA)

Table 1 shows the total 15 runs and two responses of the Doehlert design. The two responses, uranium adsorption capacity (q) and removal efficiency (e), ranges from 37.94 to 312.06 mg/g and 7.59 to 86.02%, respectively. The ratios of max to min are 9.28 and 11.53. If the p-value of model term was less than 0.05, this model term was considered as significant. After ANOVA, although the p-values of the model (0.0010 and 0.0024) were significant, but the p-values of lack-of-fit (0.0311 and 0.0119) were also significant. The significant p-values of lack-of-fit meant that there might be some systematic variation unaccounted for in the model.

Therefore, Y' was defined as the transformation of response to diminish the ratios of max to min and keep the predicted responses beyond zero. The transformation from Y to Y' was according to the following equation:

$$Y' = \ln(Y) \quad (10)$$

where Y' is the transformation of response, and Y is the response.

After transformation, the model F-value (357.56) and lower p-value (<0.0001) of adsorption capacity (659.34 and <0.0001 for removal efficiency) implied the regressional models were statistically significant. The p-values of lack-of-fit (0.1327 and 0.1829) implied the lack-of-fit was not significant and the model was well fitted for the responses. The R^2 at values 0.9984 and 0.9991 of two responses were much higher than 0.95 and very close to 1.0000. All of the ANOVA results illustrated good agreement between the predicted and observed results in the range of experiment.

In this case X_1, X_2, X_3, X_1X_2, X_2X_3, X_1^2 and X_2^2 were significant model terms for adsorption capacity, and X_1, X_2, X_3, X_1X_2, X_1X_3, X_2X_3, X_1^2 and X_3^2 were significant model terms for removal efficiency. The relationship between the independent variables

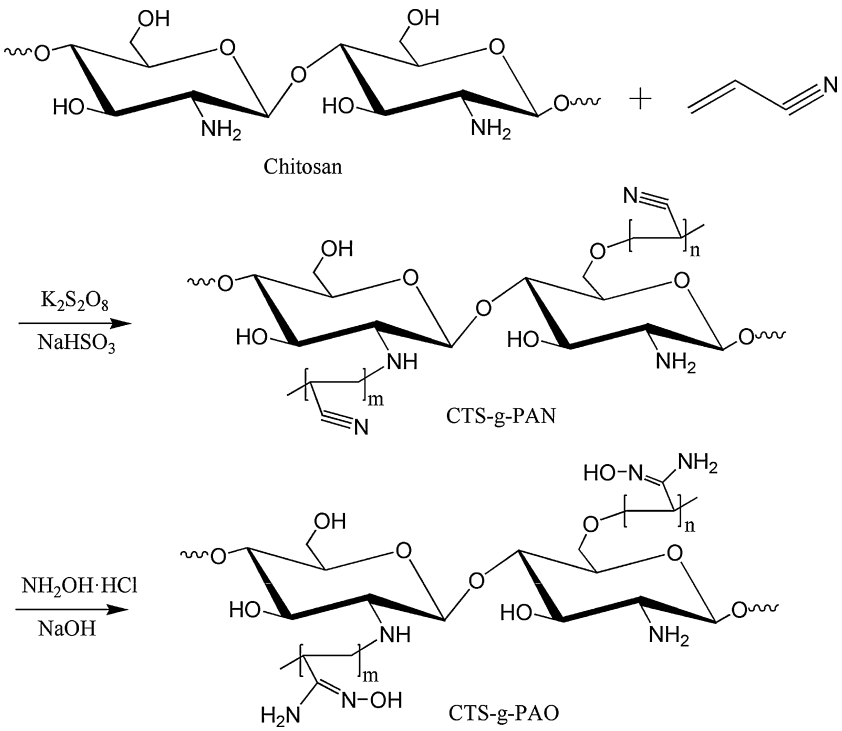

Fig. 1. The process for the preparation of CTS-*g*-PAO.

and adsorption capacity was expressed by the following quadratic equation:

$$\begin{aligned}\mathrm{Ln}(Y_1) = {} & -7.29817 + 3.28106X_1 + 0.063582X_2 + 3.82223X_3 \\ & - 1.31829E-003\,X_1X_2 + 0.68721X_1X_3 - 0.15077X_2X_3 \\ & - 0.24639X_1^2 - 3.03784E-004X_2^2 - 19.79136X_3^2 \end{aligned} \quad (11)$$

For removal efficiency, the relationship could be descriped by the following quadratic equation:

$$\begin{aligned}\mathrm{Ln}(Y_2) = {} & -8.4874 + 3.28106X_1 + 0.015732X_2 + 26.73670X_3 \\ & - 1.31829E-003X_1X_2 + 0.68721X_1X_3 - 0.14569X_2X_3 \\ & - 0.24639X_1^2 - 5.58471E-005X_2^2 - 80.09627X_3^2 \end{aligned} \quad (12)$$

where X_1 is initial pH, X_2 is initial concentration of uranium and X_3 is the solid–liquid ratio.

3.2.2. Effect of initial pH and concentration

Due to the quadratic polynomial equation of RSM (Eqs. (11) and (12)), the effects of these three independent variables on the UO_2^{2+} adsorption capacity and removal efficiency were analyzed.

The 3D surface graphs shown in Fig. 2 display the variation of adsorption capacity and removal efficiency based on the increase of initial pH and concentration. When the solid–liquid ratio is constant at 0.050 g/l, the UO_2^{2+} adsorption capacity varied from 17.07 to 343.22 mg/g (Fig. 2a). The adsorption capacity increased with the increase of initial concentration and pH (beneath 7.0). The adsorption capacity increased faster with pH closer to 7.0. However, it decreased when pH was beyond 7.0. When pH was 9.4 or concentration was beyond 70 mg/l, the adsorption capacity increased slowly. When pH was between 5.8 and 7.2 and the concentration was beyond 65 mg/l, the adsorption capacity could attain 300 mg/g.

In Fig. 2b, the UO_2^{2+} removal efficiency varied from 4.19 to 105.07%, when the solid–liquid ratio was constant at 150 mg/l. The removal efficiency increased with decrease of concentration, which was contrary to adsorption capacity. It increased when pH increased from 4.6 to nearly 7.0, then decreased when pH continully increased to 9.4, same to adsorption capacity. When pH was between 6.2 and 7.5 and the concentration was beneath 30 mg/l, the removal efficiency could attain 85%.

The UO_2^{2+} ions have many kinds of uranyl complexes in natural water, such as $(UO_2)_2(OH)_2^{2+}$, $(UO_2)_3(OH)_5^{+}$, UO_2OH^{+}, $UO_2(CO_3)_2^{2-}$, $UO_2(CO_3)_3^{4-}$, $UO_2CO_3^0$ and so on (Farrell, Bostick, Jarabek, & Fiedor, 1999; Raff & Wilken, 1999). When pH was between 6 and 7, $UO_2(CO_3)_2^{2-}$ and $UO_2CO_3^0$ were the main complexes. There were little $(UO_2)_3(OH)_5^{+}$ and UO_2OH^{+} in the same pH condition. The $-NH_2$ was the main function group of CTS-*g*-PAO and would be turned to $-NH_3^{+}$ on the condition of faintly acid. The amount of $UO_2(CO_3)_2^{2-}$ complex highly increased at pH = 6, and decreased at pH = 7. So $UO_2(CO_3)_2^{2-}$ seemed to be the key complexes which would have reactions with CTS-*g*-PAO. That might explain why pH was extremely significant model terms (p-values <0.0001) for both adsorption capacity and removel efficiency.

3.2.3. Effect of initial pH and solid–liquid ratio

The uranium adsorption capacity and removal efficiency of CTS-*g*-PAO based on the increase of initial pH and solid–liquid ratio at a constant initial concentration were also analyzed (Fig. 3). The adsorption capacity varied from 24.81 to 342.86 mg/g, while the initial concentration was constant at 80 mg/l (Fig. 3a). In Fig. 3b, the removal efficiency varied from 3.75 to 105.08%, while the initial concentration was constant at 20 mg/l. Both of the two responses increased when pH increased from 4.6 to nearly 7.0, then decreased when pH continully increased to 9.4. The effect of solid–liquid ratio was contrary to the effect of initial concentration. With the increase of solid–liquid ratio, adsorption capacity decreased, however removal efficiency increased. When pH was closer to 7.0, these two responses varied faster.

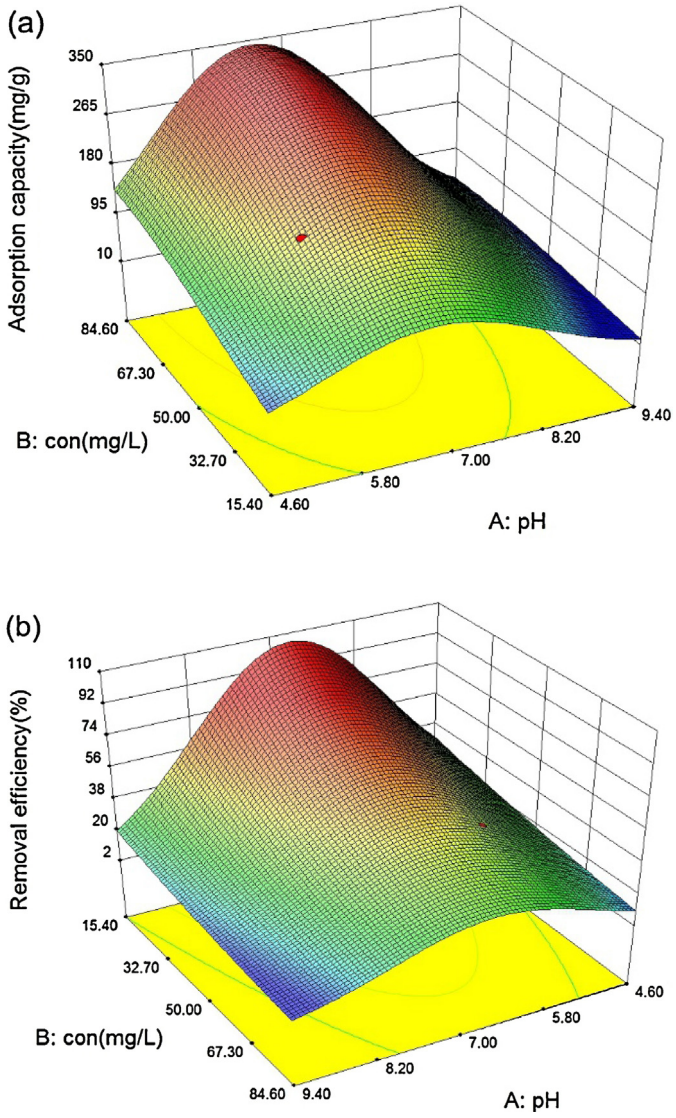

Fig. 2. The effect of initial pH and initial concentration on UO_2^{2+} adsorption capacity and removal efficiency (con: initial concentration of uranium; *s–l* ratio: solid–liquid ratio; (a) adsorption capacity, *s–l* ratio = 50 mg/l; (b) removal efficiency, *s–l* ratio = 150 mg/l).

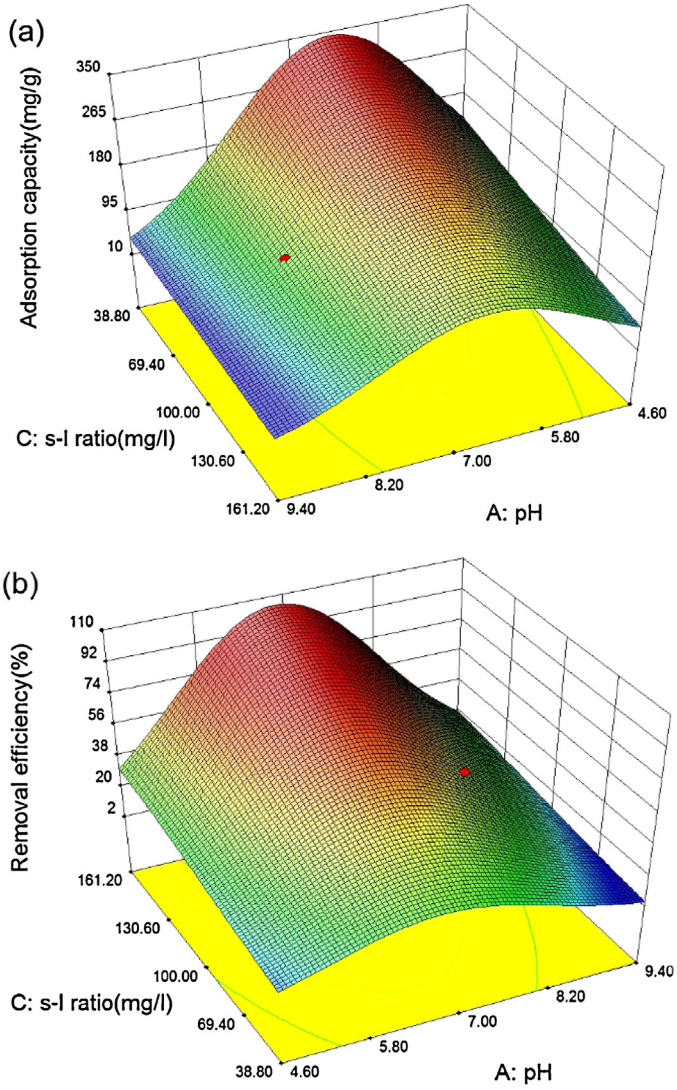

Fig. 3. The effect of initial pH and solid–liquid ratio on UO_2^{2+} adsorption capacity and removal efficiency (con: initial concentration of uranium; *s–l* ratio: solid–liquid ratio; (a) adsorption capacity, con = 80 mg/l, (b) removal efficiency, con = 20 mg/l).

When pH was between 6.0 and 7.0 and solid–liquid ratio was beneath 65 mg/l, the adsorption capacity could reach 300 mg/g. When pH was between 6.0 and 7.5 and solid–liquid ratio was beyond 130 mg/l, the removal efficiency could reach 85%.

3.2.4. *Effect of initial concentration and solid–liquid ratio*

In Fig. 4, the 3D surface graphs express the variation of uranium adsorption capacity and removal efficiency based on the increase of initial concentration and solid–liquid ratio, when the initial pH was constant at 7.0. The adsorption capacity and removal efficiency varied from 120.67 to 323.54 mg/g and 20.14 to 104.19%, respectively. The adsorption capacity and the increase rate of itself rose with the decrease of the initial concentration and the increase of solid–liquid ratio (Fig. 4a). On the contrary, the removal efficiency and the increase rate of itself rose with the increase of the initial concentration and the decrease of solid–liquid ratio (Fig. 4b).

When the solid–liquid ratio was beneath 63 mg/l and the initial concentration was beyond 65 mg/l, the adsorption capacity would achieve 300 mg/g. When the solid–liquid ratio was beyond 130 mg/l and the initial concentration was beneath 30 mg/l, the removal efficiency would achieve 85%.

3.3. *Desorption and regeneration*

The adsorbed uranium by CTS-*g*-PAO would be effectively eluted by ether 0.1 mol/l HCl or 0.1 mol/l EDTA-Na aqueous solutions. More than 80% of adsorbed uranium could be recycled (Table 2). While the untreated chitosan could be dissolved in both 0.1 mol/l HCl and 0.1 mol/l EDTA-Na solutions. The amidoximated polyacrylonitrile (PAO), which did not graft chitosan, could be dissolved in

Table 2
Desorption and regeneration of CTS-*g*-PAO.

Run times	HCl			EDTA-Na		
	q (mg/g)	R_1 (%)	R_2 (%)	*q* (mg/g)	R_1 (%)	R_2 (%)
1	224.46	88.52		225.99	92.97	
2	200.00	85.43	89.90	186.85	87.27	81.96
3	197.79	81.63	88.91	185.73	80.67	81.46

q: adsorption capacity; R_1: uranium recycle efficiency; R_2: material regeneration efficiency.

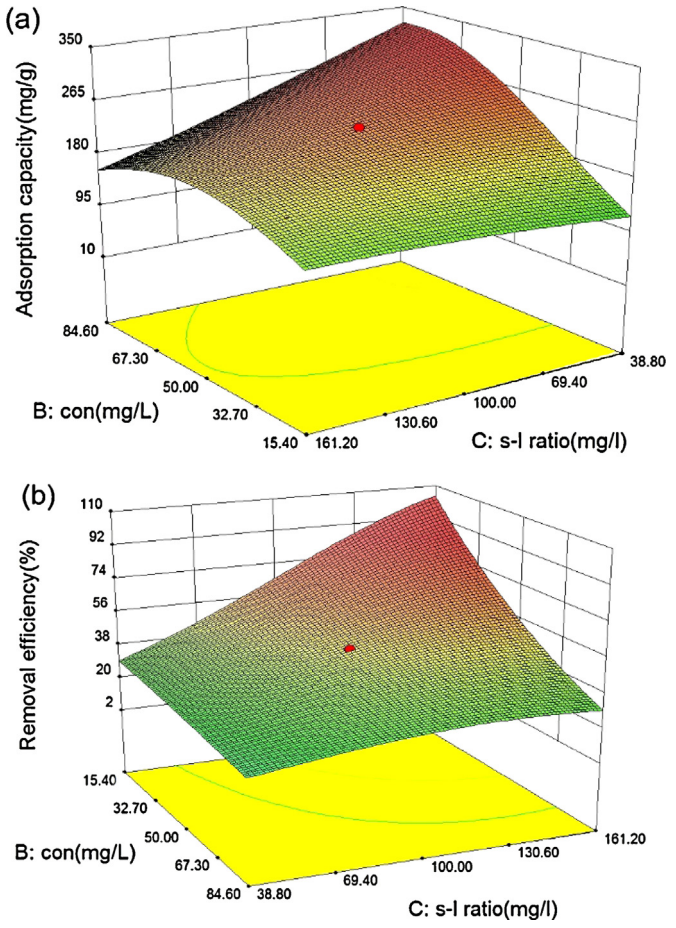

Fig. 4. The effect of initial concentration and solid–liquid ratio on UO_2^{2+} adsorption capacity and removal efficiency (con: initial concentration of uranium; *s–l* ratio: solid–liquid ratio; (a) adsorption capacity, pH = 7.0; (b) removal efficiency, pH = 7.0).

0.1 mol/l HCl solution. CTS-*g*-PAO has better insolubility properties than chitosan and PAO.

Besides, CTS-*g*-PAO could be used at least three times (Table 2). At thirst time, the uranium adsorption capacity could retain more than 81% (more than 88% for HCl) of the capacity at first time. CTS-*g*-PAO would have more practical applications.

3.4. Scanning electron microscopy (magnification ×5000)

The surface morphology of Chitosan, CTS-*g*-PAO and CTS-*g*-PAO after adsorption of uranium is illustrated in Fig. 5. It is obvious that the grafting and amidoximation totally modified the surface morphology of Chitosan. The micrograph of Chitosan, as shown in Fig. 5a, revealed its fibrous and flaky nature. While the fibrous and flaky nature was modified by lots of irregular lumps and holes in the surface of CTS-*g*-PAO. In Fig. 5c, there appeared numerous flaky uranyl crystals which were originally adsorbed by CTS-*g*-PAO. The crystal might crystalize in the filtration and drying process. These obvious changes in the scanning electron micrographs provided additional proofs for the preparation as well as adsorption.

3.5. Adsorption isotherm

Langmuir and Freundlich models were used for isotherm studies (Azizian, 2004; Foo & Hameed, 2010). The isotherm equations are shown as below:

$$\text{Langmuir}: \frac{C_e}{q_e} = \frac{1}{(b_L q_0)} + \frac{C_e}{q_0} \quad (13)$$

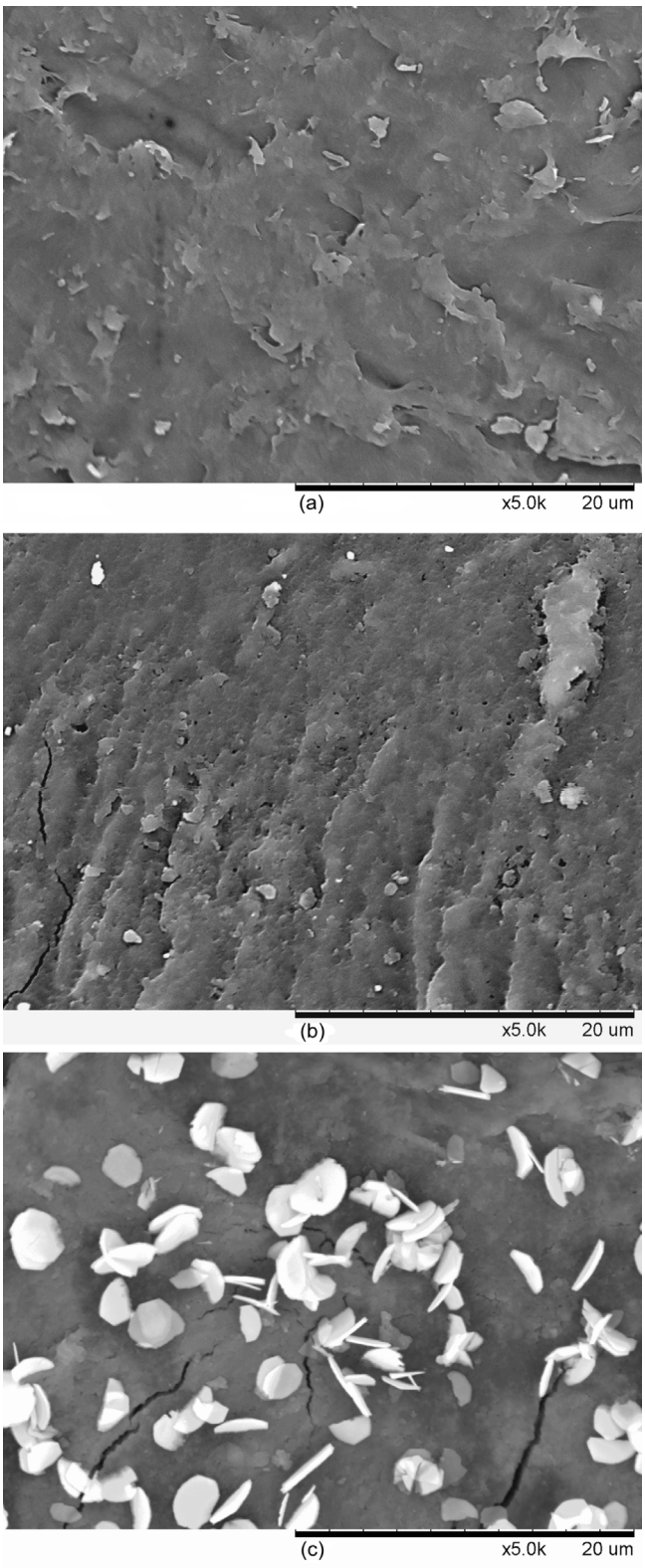

Fig. 5. Scanning electron micrographs of chitosan (a), CTS-*g*-PAO (b) and CTS-*g*-PAO after adsorption of uranium (c).

$$\text{Freundlich}: \ln(q_e) = \ln(k_F) + b_F \ln(C_e) \quad (14)$$

where C_e is the equilibrium concentration (mg/l), q_e is the adsorption capacity at equilibrium (mg/g), q_0 is the maximum adsorption capacity (mg/g), b_L is the Langmuir isotherm constant (l/mg), and k_F is the Freundlich isotherm constant (mg/g).

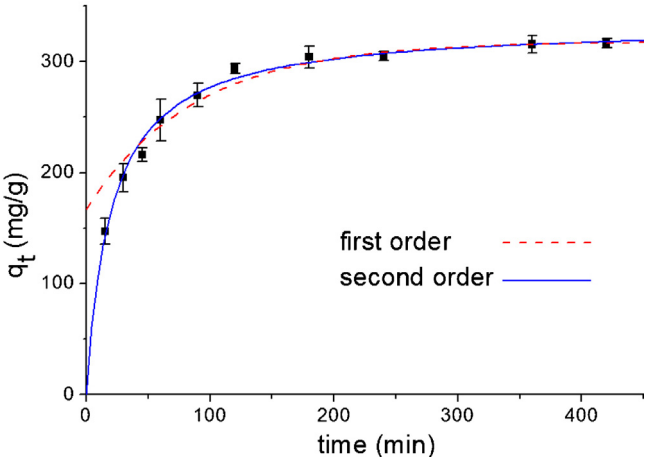

Fig. 6. Pseudo first order and second order kinetic profiles of the adsorption.

The adsorption capacities of different initial concentrations (15, 30, 45, 70 and 80 mg/l) were investigated in condition of pH = 7 and solid–liquid ratio = 100 mg/l. It was found that Freundlich model (R^2 = 0.8906) could not well describe the adsorption progress. Langmuir model was more reliable (R^2 = 0.9845).

3.6. Adsorption kinetics

The pseudo first order and second order kinetic models were used for kinetic studies (Azizian, 2004). The kinetic equations are shown as below:

$$\text{Pseudo first order}: \ln(q_e - q_t) = 0 \ln q_e - k_1 t \quad (15)$$

$$\text{Pseudo second order}: \frac{t}{q_t} = \frac{1}{\left(k_2 q_e^2\right)} + \frac{t}{q_e} \quad (16)$$

where t is the time (min), q_e is the adsorption capacity at equilibrium (mg/g), q_t is adsorption capacity at t minutes (mg/g), k_1 is the pseudo first order kinetic constant (min^{-1}), and k_2 is the pseudo second order kinetic constant (g/(min·mg)).

The adsorption capacities of different times were investigated in condition of pH = 7, initial concentration = 85 mg/l and solid–liquid ratio = 50 mg/l. The kinetic fitting results are shown in Fig. 6. The adsorption process would reach equilibrium less in 120 min. Both pseudo first and second order kinetic models well described the adsorption progress (R^2 > 0.95), and the pseudo second order kinetic model (R^2 = 0.9997) was more suitable than first order (R^2 = 0.9752).

4. Conclusion

In this research, CTS-*g*-PAO was prepared by graft copolymerization and amidoximation reactions for the adsorption of uranium from aqueous medium. The adsorption was optimized by the Doehlert design of response surface methodology (model p-value <0.0001, R^2 = 0.99 and lack-of-fit p-value >0.05). The CTS-*g*-PAO could achieve considerable uranium adsorption capacity (312.06 mg/g) and removal efficiency (86.02%). The pH, concentration of uranium, solid–liquid ratio and some of their interactions had significant effects on the adsorption.

Moreover, most of the adsorbed uranium could be desorbed by ether 0.1 mol/l HCl or EDTA-Na solutions, and CTS-*g*-PAO could be reused at least three times. The FTIR analysis indicated that uranyl ions was bonded to amidoxime and amino group by chelation. The adsorption process would reach equilibrium in 120 min, and was very suitable for Langmuir isotherm model (R^2 = 0.98) and pseudo second order kinetics model (R^2 = 0.99).

The obtained results revealed that CTS-*g*-PAO had better physical and adsorption properties than chitosan and amidoximated polyacrylonitrile. It would have well practical application prospects in uranium removal from contaminated water and extraction from sea water.

Acknowledgement

This work was supported by "Special Fund for Agro-scientific Research in the Public Interest (201103007)".

References

Amini, M., Younesi, H., & Bahramifar, N. (2009). Biosorption of nickel(II) from aqueous solution by *Aspergillus niger*: Response surface methodology and isotherm study. *Chemosphere*, *75*(11), 1483–1491.
Anirudhan, T. S., & Radhakrishnan, P. G. (2009). Improved performance of a biomaterial-based cation exchanger for the adsorption of uranium(VI) from water and nuclear industry wastewater. *Journal of Environmental Radioactivity*, *100*(3), 250–257.
Azizian, S. (2004). Kinetic models of sorption: A theoretical analysis. *Journal of Colloid and Interface Science*, *276*(1), 47–52.
Bezerra, M. A., Santelli, R. E., Oliveira, E. P., Villar, L. S., & Escaleira, L. A. (2008). Response surface methodology (RSM) as a tool for optimization in analytical chemistry. *Talanta*, *76*(5), 965–977.
Doehlert, D. H. (1970). Uniform shell designs. *The Royal Statistical Society Series C—Applied Statistics*, *19*(3), 231–239.
Dotto, G. L., & Pinto, L. A. A. (2011). Adsorption of food dyes onto chitosan: Optimization process and kinetic. *Carbohydrate Polymers*, *84*(1), 231–238.
Farrell, J., Bostick, W. D., Jarabek, R. J., & Fiedor, J. N. (1999). Uranium removal from ground water using zero valent iron media. *Ground Water*, *37*(4), 618–624.
Foo, K. Y., & Hameed, B. H. (2010). Insights into the modeling of adsorption isotherm systems. *Chemical Engineering Journal*, *156*(1), 2–10.
Gao, B., Gao, Y., & Li, Y. (2010). Preparation and chelation adsorption property of composite chelating material poly(amidoxime)/SiO_2 towards heavy metal ions. *Chemical Engineering Journal*, *158*(3), 542–549.
Jayakumar, R., Prabaharan, M., Reis, R. L., & Mano, J. F. (2005). Graft copolymerized chitosan—Present status and applications. *Carbohydrate Polymers*, *62*(2), 142–158.
Kumar, R., Singh, R., Kumar, N., Bishnoi, K., & Bishnoi, N. R. (2009). Response surface methodology approach for optimization of biosorption process for removal of Cr(VI), Ni(II) and Zn(II) ions by immobilized bacterial biomass sp. *Bacillus brevis*. *Chemical Engineering Journal*, *146*(3), 401–407.
Lv, P., Bin, Y., Li, Y., Chen, R., Wang, X., & Zhao, B. (2009). Studies on graft copolymerization of chitosan with acrylonitrile by the redox system. *Polymer*, *50*(24), 5675–5680.
Mohamed, R. R., & Sabaa, M. W. (2010). Graft copolymerization of acrylonitrile and its amidoxime derivative onto chitosan. *Journal of Applied Polymer Science*, *116*(1), 413–421.
Muzzarelli, R. A. A. (2011). Potential of chitin/chitosan-bearing materials for uranium recovery: An interdisciplinary review. *Carbohydrate Polymers*, *84*(1), 54–63.
Ning, Y.-C. (2000). *Structural identification of organic compounds and organic spectroscopy*. Beijing: Science Press.
Oshita, K., Sabarudin, A., Takayanagi, T., Oshima, M., & Motomizu, S. (2009). Adsorption behavior of uranium(VI) and other ionic species on cross-linked chitosan resins modified with chelating moieties. *Talanta*, *79*(4), 1031–1035.
Raff, O., & Wilken, R.-D. (1999). Removal of dissolved uranium by nanofiltration. *Desalination*, *122*(2–3), 147–150.
Rinaudo, M. (2006). Chitin and chitosan: Properties and applications. *Progress in Polymer Science (Oxford)*, *31*(7), 603–632.
Saraydin, D., Isikver, Y., & Sahiner, N. (2001). Uranyl ion binding properties of poly(hydroxamic acid) hydrogels. *Polymer Bulletin*, *47*(1), 81–89.
Schleuter, D., Günther, A., Paasch, S., Ehrlich, H., Kljajić, Z., Hanke, T., et al. (2013). Chitin-based renewable materials from marine sponges for uranium adsorption. *Carbohydrate Polymers*, *92*(1), 712–718.
Shankar, P., Gomathi, T., Vijayalakshmi, K., & Sudha, P. N. (2014). Comparative studies on the removal of heavy metals ions onto cross linked chitosan-*g*-acrylonitrile copolymer. *International Journal of Biological Macromolecules*, *67*(0), 180–188.
Shen, J., Lin, L., Chen, W., Zhou, Y., & Jin, K. (2011). Recent development of uranium extraction materials from sea-water. *Chemical Industry and Engineering Progress*, *30*(12), 2586–2592.
Varma, A. J., Deshpande, S. V., & Kennedy, J. F. (2004). Metal complexation by chitosan and its derivatives: A review. *Carbohydrate Polymers*, *55*(1), 77–93.
Wan Ngah, W. S., Teong, L. C., & Hanafiah, M. A. K. M. (2011). Adsorption of dyes and heavy metal ions by chitosan composites: A review. *Carbohydrate Polymers*, *83*(4), 1446–1456.
Wang, J.-s., Peng, R.-t., Yang, J.-h., Liu, Y.-c., & Hu, X.-j. (2011). Preparation of ethylenediamine-modified magnetic chitosan complex for adsorption of uranyl ions. *Carbohydrate Polymers*, *84*(3), 1169–1175.